Available online at www.sciencedirect.com
ScienceDirect
Geomorphology 94 (2008) 268–289
GEOMORPHOLOGY
www.elsevier.com/locate/geomorph

Comparing landslide inventory maps

Mirco Galli, Francesca Ardizzone, Mauro Cardinali, Fausto Guzzetti *, Paola Reichenbach

CNR-IRPI, via della Madonna Alta 126, 06128 Perugia, Italy

Received 15 July 2005; received in revised form 25 February 2006; accepted 9 September 2006
Available online 14 June 2007

Abstract

Landslide inventory maps are effective and easily understandable products for both experts, such as geomorphologists, and for non experts, including decision-makers, planners, and civil defense managers. Landslide inventories are essential to understand the evolution of landscapes, and to ascertain landslide susceptibility and hazard. Despite landslide maps being compiled every year in the word at different scales, limited efforts are made to critically compare landslide maps prepared using different techniques or by different investigators. Based on the experience gained in 20 years of landslide mapping in Italy, and on the limited literature on landslide inventory assessment, we propose a general framework for the quantitative comparison of landslide inventory maps. To test the proposed framework we exploit three inventory maps. The first map is a reconnaissance landslide inventory prepared for the Umbria region, in central Italy. The second map is a detailed geomorphological landslide map, also prepared for the Umbria region. The third map is a multi-temporal landslide inventory compiled for the Collazzone area, in central Umbria. Results of the experiment allow for establishing how well the individual inventories describe the location, type and abundance of landslides, to what extent the landslide maps can be used to determine the frequency-area statistics of the slope failures, and the significance of the inventory maps as predictors of landslide susceptibility. We further use the results obtained in the Collazzone area to estimate the quality and completeness of the two regional landslide inventory maps, and to outline general advantages and limitations of the techniques used to complete the inventories.

Keywords: Landslide map; Inventory; Density; Susceptibility; Map comparison; Umbria

1. Introduction

Landslides play an important role in the evolution of landforms (Harmon and Doe, 2001), and represent a serious hazard in many areas of the World (Brabb and Harrod, 1989). Several investigators have attempted to identify landslides and to produce landslide maps. Depending on the purpose and the available resources, landslide inventory maps are compiled at different scales, from the local to the national, using a variety of techniques, including the analysis of stereoscopic aerial photographs, geomorphological field mapping, engineering-geological slope investigations, and the examination of historical archives (Guzzetti et al., 2000). A combination of these techniques is often used.

Landslide inventory maps are prepared for different purposes, including: (i) showing the location and type of landslides in a region (Antonini et al., 1993; Cardinali et al., 2001; Antonini et al., 2002a), (ii) showing the

* Corresponding author. Tel.: +39 075 5014421; fax: +39 075 5014420.
E-mail address: Mirco.Galli@irpi.cnr.it (M. Galli).

0169-555X/$ - see front matter © 2007 Elsevier B.V. All rights reserved.
doi:10.1016/j.geomorph.2006.09.023

effects of single landslide triggering events, such as an earthquake (Harp and Jibson, 1995, 1996), an intense rainfall event (Bucknam et al., 2001) or a rapid snowmelt event (Cardinali et al., 2000), (iii) showing the abundance of mass movements (DeGraff, 1985; DeGraff and Canuti, 1988; Guzzetti et al., 2000), (iv) determining the frequency-area statistics of slope failures (Hovius et al., 1997, 2000; Guzzetti et al., 2002; Brardinoni et al., 2003; Guthrie and Evans, 2004a,b; Malamud et al., 2004), and (v) providing relevant information to construct landslide susceptibility (Soeters and van Westen, 1996; Guzzetti et al., 1999; Chung and Fabbri, 1999, 2003, 2005) or hazard (Guzzetti et al., 2005, 2006a,b) models. The quality and completeness of the landslide maps affects the reliability of the estimates obtained from the inventories. Determining the quality of the landslide inventories is, therefore, important.

Absolute criteria to establish the quality of a landslide inventory map have not been established. Most commonly, the quality of an inventory is ascertained in relative terms, i.e., by comparison with other inventories. In this paper, we establish the quality of two

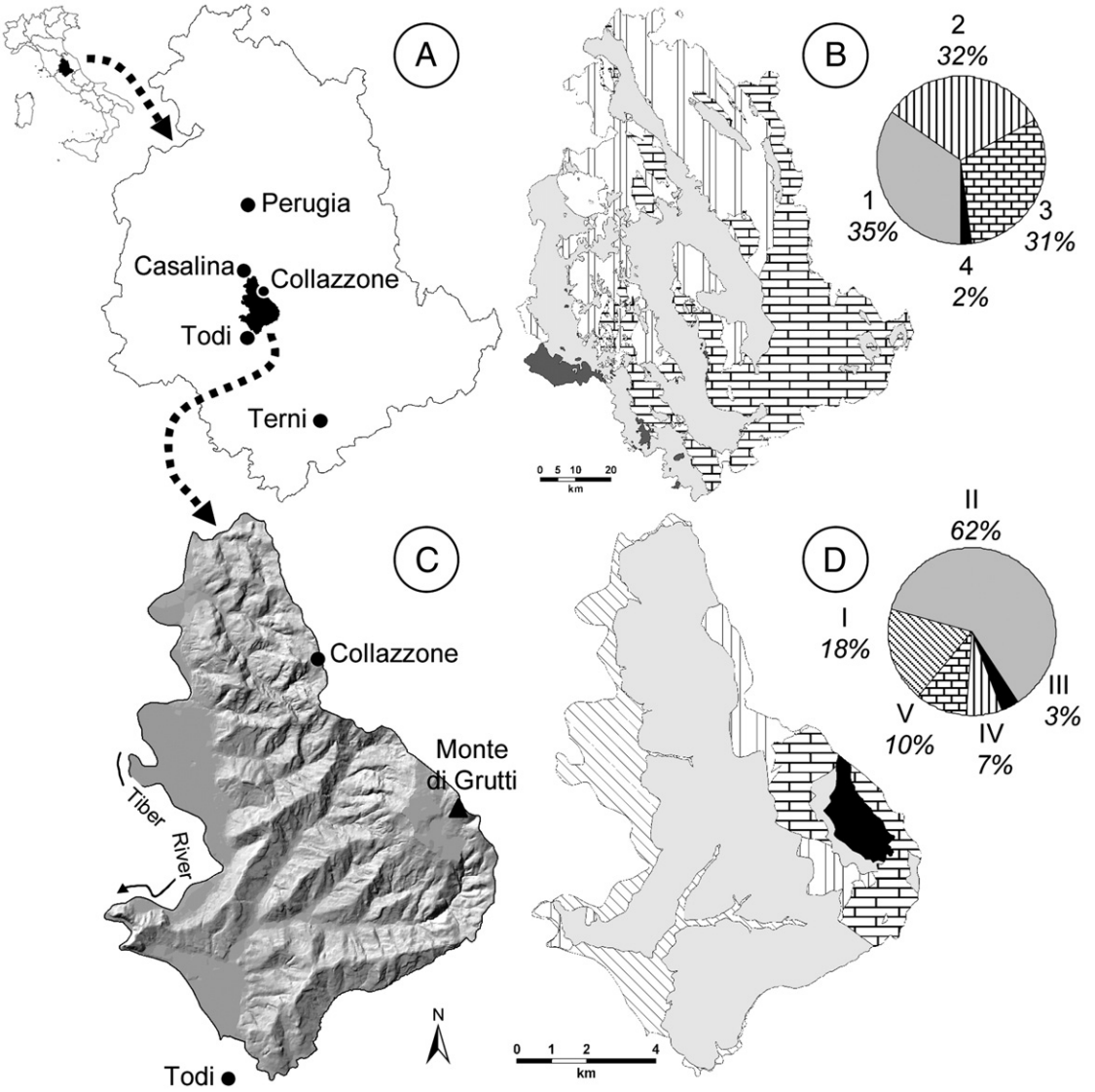

Fig. 1. Location map. (A) Umbria region. Black area shows location of the Collazzone study area. (B) Simplified lithological map for the Umbria region. Modified after Servizio Geologico d'Italia (1980) and Cardinali et al. (2001). (1) Marine and lake deposits; (2) flysch deposits; (3) carbonate rocks; (4) volcanic rocks. (C) Shaded relief image for the Collazzone area. (D) Lithological map for the Collazzone area. (I) Alluvial deposits, Holocene in age; (II) continental deposits, Plio–Pleistocene in age; (III) travertine, Pleistocene in age; (IV) layered sandstone and marl, Miocene in age; (V) thinly layered limestone, Lias to Oligocene in age.

landslide maps prepared for the Umbria region, in central Italy, and of a multi-temporal landslide map prepared for the Collazzone area, in central Umbria (Fig. 1). We accomplish this by systematically comparing the three maps. The comparison is aimed at establishing how well the three inventories: (i) describe the location, type, and abundance of the landslides, (ii) determine the statistics of landslide areas, and (iii) provide reliable information to construct landslide susceptibility models.

2. The study area

The Umbria region lies along the Apennines Mountain chain in central Italy, and covers an area of 8456 km^2, with elevation ranging from 50 to 2436 m (Fig. 1A). In the area climate is Mediterranean, with distinct wet and dry seasons. Four major rock and sediment types are present (Fig. 1B): (i) carbonate rocks, comprising layered and massive limestone, cherty limestone and marl, (ii) flysch deposits, comprising layered sandstone, marl, shale and clay, (iii) volcanic rocks, encompassing lava flows, ignimbrites and pyroclasitc deposits, and (iv) marine and continental sediments made up of clay, silty clay, fine and coarse sand, gravel and cobbles (Servizio Geologico Nazionale, 1980). Due to the morphological, geological and climatic settings, landslides are abundant in Umbria and cover about 8% of the territory (Guzzetti et al., 1996, 2003).

The Collazzone area extends for about 90 km^2 in central Umbria, with elevations ranging from 145 m along the Tiber River flood plain to 634 m at Monte di Grutti (Fig. 1C). The rock and sediment in this area include (Fig. 1D): (i) fluvial deposits along the main valley bottoms, (ii) continental gravel, sand and clay, (iii) travertine, (iv) layered sandstone and marl, and (v) thinly layered limestone (Conti and Girotti, 1977; Servizio Geologico Nazionale, 1980; Cencetti, 1990; Barchi et al., 1991). The terrain is hilly, valleys are asymmetrical, and slopes are controlled by lithology and the attitude of bedding. Annual rainfall averages 884 mm, and is most abundant in the period from September to December (Fig. 2). Mass movements are abundant in the area, and range in type and volume from large translational slides to deep and shallow flows.

In this study we consider the hilly portion of the Collazzone area that extends for 78.89 km^2.

3. Landslide inventory maps

Two landslide inventory maps have been made for the Umbria region. The first map is a reconnaissance inventory prepared by Guzzetti and Cardinali (1989) (Fig. 3A). The second map is a geomorphological inventory prepared by Antonini et al. (2002a) (Fig. 3B). For the Collazzone area, a detailed multi-temporal landslide inventory map was prepared in 2002 and updated in 2003 and 2004 (Fig. 4).

3.1. Reconnaissance geomorphological inventory map

The first landslide inventory map to cover the Umbria region was prepared by Guzzetti and Cardinali in 1987 and 1988 (Fig. 3A) as a reconnaissance mapping effort aimed at obtaining general information on the distribution, abundance and type of mass movements in Umbria. In 1999, the Regional Government of Umbria adopted the map as part of the Regional Environmental and Urban Plan.

The reconnaissance inventory was prepared by interpreting landslides observed on 1085 pancromatic, vertical aerial photographs flown in the period from 1954 to 1956, at 1:33,000 scale (Table 1). Interpretation of the aerial photographs was locally aided by field checks, and was carried out by a team of two geomorphologists who worked simultaneously on adjacent strips. Inasmuch as side-lap between the photographs was 20–30%, a considerable part of the territory was analysed by both photo-interpreters. The landslide information, originally plotted on transparent plastic sheets placed over the aerial photographs, was transferred to 35 topographic maps, at 1:25,000 scale. Transfer of the landslide information to the base maps was accomplished by using a combined optical and manual technique, aided by a large-format photographic projector. The 35 quadrangles were then

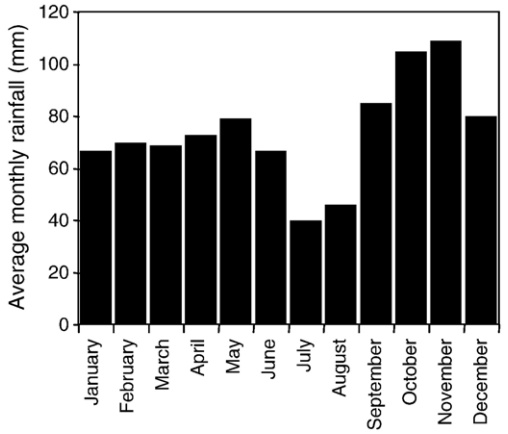

Fig. 2. Collazzone area. Average monthly rainfall for the period between 1921 and 2001 for the Casalina rain gauge.

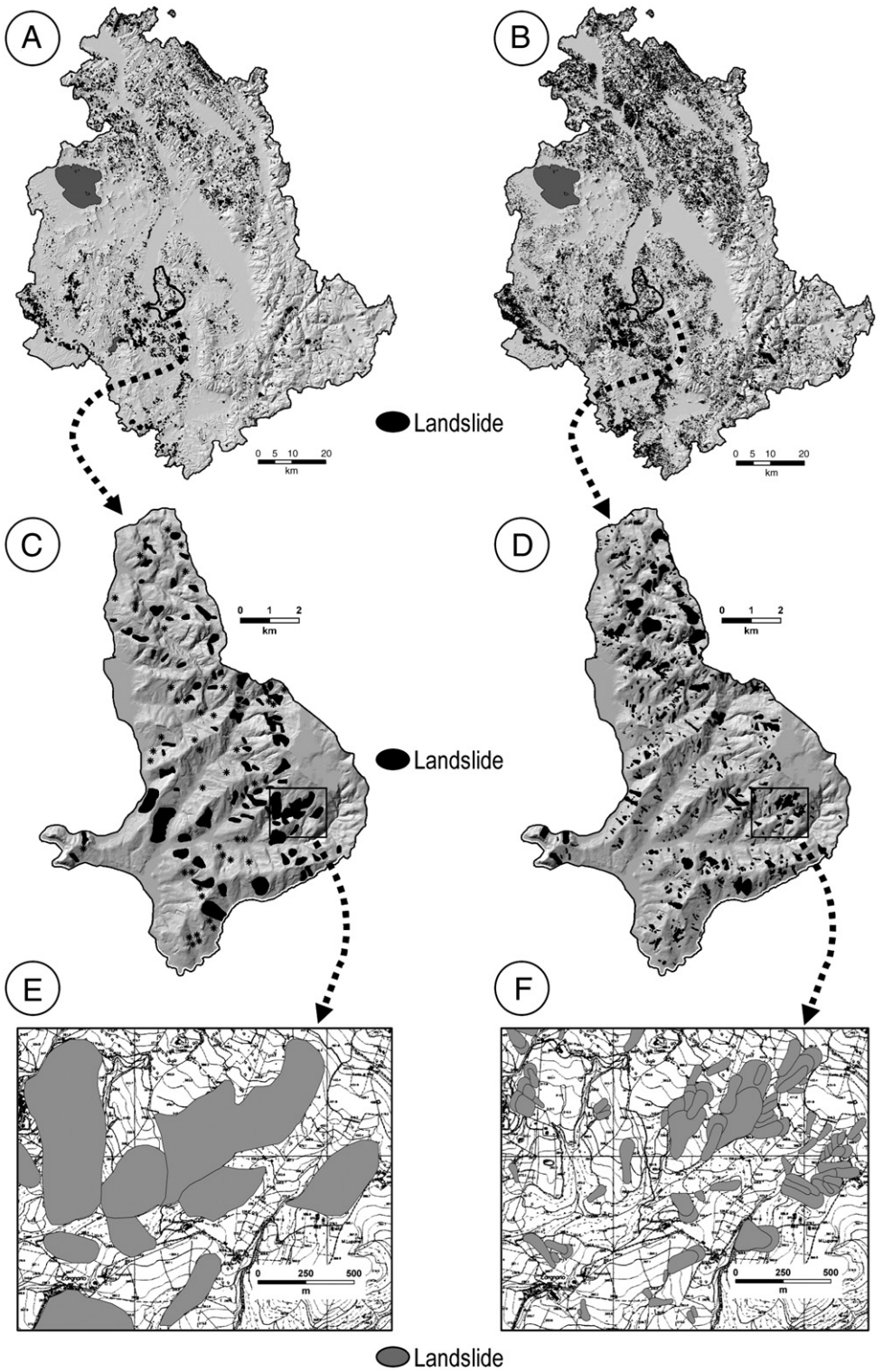

Fig. 3. Landslide inventory maps for the Umbria region. (A) Reconnaissance inventory map (Guzzetti and Cardinali, 1989, 1990); (B) Geomorphological inventory map (Antonini et al., 2002a); (C) Portion of the reconnaissance inventory for the Collazzone area. (D) Portion of the geomorphological inventory for the Collazzone area. (E) Enlargement of (C). (F) Enlargement of (D).

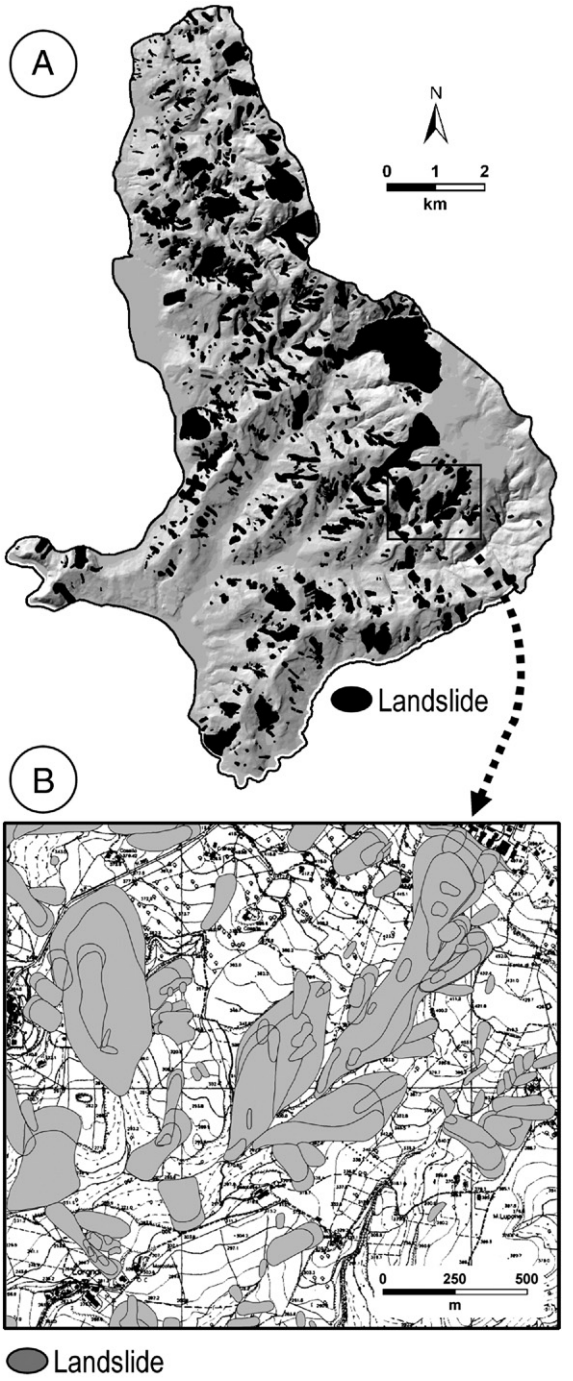

Fig. 4. Collazzone area. (A) Multi-temporal landslide inventory map prepared through the interpretation of 5 sets of aerial photographs. (B) Enlargement.

photographically reduced, assembled, and redrawn for final publication at 1:100,000 scale. Due to the scale of the published map, individual landslides with an area less than about 1 ha were shown as points in the final inventory map.

Mapping of the landslides took 9 months, for an average of about 470 km^2 per interpreter per month (Table 2). To obtain a digital version of the reconnaissance inventory map, the line work used to publish the map was scanned with a large format cartographic scanner. The raster representation of the geomorphological images was then changed into vector format using a semi-automatic procedure, which allowed assigning attributes to each line segment and to each point. Polygons were then constructed and labelled with appropriate codes. Preparation of the landslide digital cartographic database took about 2 months of a GIS specialist (Table 2).

In the reconnaissance inventory map, landslides were classified by their prevalent type of movement. For this purpose, a simplified version of the Varnes (1978) classification of mass movements was used. Landslides were classified as: (i) rock fall, (ii) rotational slide, (iii) translational slide, (iv) debris flow, debris slide or debris avalanche, and (v) complex slide, including earth flow. A separate class was used to show landslides for which the type of movement was undetermined. An additional class was adopted to identify hummocky topography and areas where no landslides were clearly recognized, but where morphological, geological and vegetation elements suggested the possible or probable presence of one or several slope failures. The reconnaissance landslide map also showed major escarpments, badlands and alluvial fans (Guzzetti and Cardinali, 1989, 1990).

Table 1
Sets of aerial photographs used to prepare landslide inventory maps in Umbria

Year	Period	Type	Nominal Scale	Type of Inventory		
				a	b	c
1941	Summer	Panchromatic	1:18,000			●●
1954–56	Spring–Summer	Panchromatic	1:33,000	●●	●●	●●
1977	Spring–Summer	Colour	1:13,000		●	●●
1985	July	Panchromatic	1:15,000			●●
1994	Unknown	Panchromatic	1:73,000		●	
1997	April	Panchromatic	1:20,000			●●

(a) Reconnaissance landslide inventory prepared by Guzzetti and Cardinali (1989, 1990) for the entire Umbria region (Fig. 3A). (b) Geomorphological landslide inventory prepared by Antonini et al. (2002a) for the entire Umbria region (Fig. 3B). (c) Multi-temporal inventory map compiled for the Collazzone area (Fig. 4). ●●, aerial photographs used systematically to identify landslides; ●, aerial photographs used in limited areas or to attribute additional information to already mapped landslides.

Table 2
Characteristics of the three inventory maps available for the Umbria region and for the Collazzone area

		Map a	Map b	Map c
Source		Guzzetti and Cardinali (1989)	Antonini et al. (2002a)	This study
Figure		Fig. 3A	Fig. 3B	Fig. 4
Type of inventory		Reconnaissance	Geomorphological	Multi-temporal
Date of inventory	Year	1987–88	1999–2001	2002 (updated 2003–4)
Area (see Fig. 1)		Umbria	Umbria	Collazzone
Area extent	km^2	8456	8456	78.89
Sets of aerial photographs		1	2 (+1)	5
Scale of aerial photographs		1:33,000	1:33,000, 1:13,000 (1:73,000)	1:13,000 to 1:33,000
Scale of topographic base map		1:25,000	1:10,000	1:10,000
Scale of final (published) map		1:100,000	1:10,000	1:10,000
Time for photo-interpretation	Month	9	28	5
Team for photo-interpretation	Interpreters	2	3	2
Rate of photo-interpretation	km^2/interpreter/month	470	101	8
Time for GIS database construction	Month	2	20	1
Team for GIS database construction	GIS specialist	1	4	1
Total number of mapped landslides	#	5270	47,414	2564
Total area affected by landslides	km^2	443.57	712.64	16.47
Percent of area affected by landslides	%	5.25	8.43	20.90
Landslide density	#/km^2	0.6	5.6	32.5
Smallest mapped landslide	m^2	3071	70	78
Largest mapped landslide	km^2	3.08	4.16	1.45
Average size of mapped landslide	m^2	84,169	~13,550	~7530
Size of most abundant landslide	m^2	~25,400	~1448	~815

In Umbria, the reconnaissance inventory shows 5270 landslide deposits, corresponding to an average density of 0.6 landslides per square kilometre (Fig. 3A). The mapped slope failures cover a total landslide area of 443.57 km^2, 5.25% of the Umbria region. Landslides range in size from 3071 m^2 to 3.08 km^2, and the most frequent landslide has an area of about 25,400 m^2 (Table 2). In the Collazzone area (0.93% of Umbria), the reconnaissance inventory shows 99 landslide polygons (1.88% of total), and 44 landslide points, the latter representing slope failures too small to be shown at the scale of the published map. Density of landslides is 1.81 slope failures per square kilometre, which reduces to 1.25 failures per square kilometre if the 44 landslide points are not considered. The total landslide area is 7.75 km^2, 9.82% of the study area, and the area of the individual landslides ranges from 12,174 m^2 to 0.62 km^2, with the most abundant failures having an area of about 32,000 m^2 (Table 3).

In the following analyses (Section 4) and in the discussion (Section 5), we refer to the portion of the reconnaissance landslide inventory map that covers the Collazzone area as “Map A”.

3.2. Detailed geomorphological inventory map

The second landslide inventory map to cover the Umbria region was compiled by Antonini et al. (2002a) in the period from June 1999 to September 2001 (Fig. 3B) as part of a larger effort aimed at a better assessment of landslide hazards and risk in Umbria (Guzzetti et al., 1996, 2003; Cardinali et al., 2000, 2001, 2002a,b; Antonini et al., 2002a,b; Reichenbach et al., 2005). In 2002, the Regional Government of Umbria adopted this map as part of the Tiber River Master Plan.

The new inventory map was compiled at 1:10,000 scale by systematically re-interpreting the 1:33,000 scale aerial photographs flown in the period between 1954 and 1956. In addition, two new sets of vertical aerial photographs, flown in 1977 at 1:13,000 scale and in 1994 at 1:73,000 scale, were used (Table 1). The first additional set was interpreted where flysch deposits and lake and continental deposits crop out (Fig. 1B). The second additional set was used to estimate the state of activity of the mapped landslides, at the date of the photographs.

Interpretation of the aerial photograph was aided by field surveys aimed at solving specific interpretation

Table 3
Statistics for the three landslide inventory maps available for the Collazzone area, Central Umbria

		Map A (Fig. 3C)	Map B (Fig. 3D)	Map C (Fig. 4)
Total number of mapped landslides	#	99 (+44)	1143	2564
Total mapped landslide area	km^2	7.75	8.60	22.14
Total area covered by landslides	km^2	7.75	8.00	16.47
Percent of landslide area	%	9.82	10.14	20.87
Landslide density	$\#/km^2$	1.25 (1.81)	14.48	32.5
Smallest mapped landslide	m^2	12,174	99	78
Largest mapped landslide	km^2	0.62	0.29	1.45
Average size of mapped landslide	m^2	78,287	7526	8634
Area of most abundant mapped landslide	m^2	~32,000	~1170	~815

Map A, portion of the reconnaissance landslide inventory prepared by Guzzetti and Cardinali (1989, 1990) covering the Collazzone area (Fig. 3C). Map B, portion of the geomorphological landslide inventory prepared by Antonini et al. (2002a) covering the Collazzone area (Fig. 3D). Map C, multi-temporal inventory map for the Collazzone area (this study) (Fig. 4).

problems. Production of the new map benefited from the experience gained in the compilation of the reconnaissance map (Fig. 3A), from information on landslide types and distribution compiled for selected areas in Umbria in the period from 1990 to 2000 (Carrara et al., 1991; Barchi et al., 1993; Toppi, 1993; Cardinali et al., 1994; Lattuada, 1996; Cardinali et al., 2000; Antonini et al., 2002b), and from the compilation of the "Photogeological and landslide inventory map for the Upper Tiber River basin" (Cardinali et al., 2001).

A team of three geomorphologists completed the interpretation of the aerial photographs over a period of 28 months, for an average of 101 km^2 per interpreter per month. Two team members looked at each pair of aerial photographs using a mirror stereoscope (with a magnification of 4×) that allowed both interpreters to map contemporaneously on the same stereo pair. The third photo-interpreter, using a continuous-zoom stereoscope with a magnification of up to 20×, independently reviewed, and where necessary updated and corrected, the interpretations of the other two, and ascertained the activity of the mapped landslides using the small scale aerial photographs flown in 1994.

The landslide information was first plotted on transparent plastic sheets placed over the aerial photographs, and then transferred to 1:10,000 scale topographic base maps. Transfer of the landslide information to the base maps was accomplished visually. The landslide information was then redrawn on stable, transparent sheets, which were individually scanned to obtain black and white, raster images of each map sheet. A scanning resolution of 300 dpi was used, which corresponds to a ground resolution of 85 cm. The raster representation of the geomorphological line images was then changed into vector format using a semi-automatic procedure that allowed assigning attributes to each line segment. Polygons were then constructed and labelled with the appropriate codes, depending on their geomorphological properties. Lastly, map sheets were collected together in a geographical database, and colour plots were prepared to test the digitisation procedure. Production of the GIS database took 24 months and was accomplished by four GIS specialists (Table 2).

In the new inventory, landslides were classified according to the type of movement (WP/WLI, 1990; Cruden and Varnes, 1996), the estimated depth, degree of activity, and mapping certainty. Landslides were classified as rock fall, rotational slide, translational slide, debris flow, complex or compound movements, and deep-seated gravitational deformation. For the deep-seated landslides, the crown area was mapped separately from the deposit. Landslide characteristics, including type of movement, depth and estimated degree of activity, were determined based on the local morphological characteristics, the appearance of the landslide on the aerial photographs, and the lithological and structural setting, including the attitude of the bedding planes with respect to the local slope. This was an innovation over the reconnaissance inventory, where landslides were identified based solely on morphological criteria.

The new inventory shows 47,414 landslides, including 1563 debris flows and 131 rock falls shown as points, for a total landslide area of 712.64 km^2, 8.43% of Umbria. Based on the new inventory, landslide density in Umbria is 5.6 slope failures per square kilometre. Mapped landslides extend in size from 70 m^2 to 4.16 km^2, with the most abundant landslides exhibiting an area of about 1450 m^2 (Table 2). In the Collazzone area, the geomorphological inventory map shows 1143 landslides (2.41% of total), corresponding to a density of 14.48 landslides per square kilometre (Fig. 3D). Total landslide area is 8.00 km^2, 10.14% of the study area. Slope failures range in area from 99 m^2 to 0.29 km^2, with the most numerous failures exhibiting an area of about 1170 m^2 (Table 3).

We refer to the portion of the new geomorphological landslide inventory map covering the Collazzone area as "Map B".

3.3. Multi-temporal inventory map

For the Collazzone area (Fig. 1C), a multi-temporal landslide inventory map was prepared at 1:10,000 scale through the interpretation of five sets of aerial photographs (Table 1) and detailed geological and geomorphological field mapping. The map was updated in the period from September 2003 to April 2004 through field surveys conducted following periods of prolonged rainfall to map the rainfall-induced landslides.

The aerial photographs used to compile the multi-temporal map cover the period from 1941 to 1997, and range in scale from 1:13,000 to 1:33,000 (Table 1). A team of two geomorphologists carried out the interpretation of the aerial photographs in the 5-month period from July to November 2002, for an average of 8 km^2 per interpreter per month. The two interpreters looked at each pair of aerial photographs using a mirror stereoscope (4× magnification) and a continue-zoom stereoscope (3× to 20× magnification). Both stereoscopes allowed the interpreters to map contemporaneously on the same stereo pair. The interpreters used all morphological, geological and landslide information available from published maps, previous work carried out in the same area (including Map A and Map B), and discussion with other geomorphologists. Care was taken in identifying areas where morphology had changed in response to mass movements, and to avoid interpretation errors due to land use modifications or to the different views provided by aerial photographs taken at different dates.

The landslide information was drawn on transparent plastic sheets placed over the aerial photographs. Depending on the local abundance and complexity of the landslides, a single sheet or multiple sheets were used to map slope failures of different ages (i.e., identified on aerial photographs of different dates). To transfer the landslide information from the aerial photographs to the base maps, at 1:10,000 scale, and to construct the GIS database, we adapted the procedure used to prepare the detailed geomorphological inventory. In the GIS database, landslides attributed to a single date (e.g., a rainfall event) or period were stored separately. Following this procedure, new and active landslides recognized, e.g. in the 1977 aerial photographs were stored in a separate layer than the landslides mapped as inactive in the same photographs. As a result, for a single set of aerial photographs, multiple layers were obtained. The procedure required intensive and time-consuming GIS work to correct topological and geographical errors. The obtained GIS database stores information on landslides attributed to 12 different dates or periods. The combination of the different layers represents the multi-temporal landslide inventory map.

In the multi-temporal inventory, landslides were classified according to the type of movement, and the

Table 4
Quantitative comparison of landslide inventory maps in the Collazzone area, Central Umbria

		Buffer size (mm)						
		No buffer	0.1	0.3	0.5	1.0	2.0	10.0
Landslide area in Map A	%	9.82	10.33	11.03	11.76	13.66	17.80	54.29
Landslide area in Map B	%	10.14	10.47	11.14	11.84	13.63	17.35	48.38
Map A ∪ Map B	%	16.91	17.44	18.52	19.62	22.46	28.38	70.08
Map A ∩ Map B	%	3.21	3.35	3.66	3.98	4.83	6.77	32.58
Mapping error, E	–	0.81	0.81	0.80	0.79	0.78	0.76	0.53
Mapping match, M	–	0.19	0.19	0.20	0.21	0.22	0.24	0.47
Landslide area in Map A	%	9.82	10.33	11.03	11.76	13.66	17.80	54.29
Landslide area in Map C	%	20.87	21.41	22.47	23.54	26.20	31.41	65.81
Map A ∪ Map C	%	25.09	25.72	26.98	28.25	31.45	37.87	77.08
Map A ∩ Map C	%	5.77	6.01	6.53	7.05	8.42	11.39	43.01
Mapping error, E	–	0.77	0.77	0.76	0.75	0.73	0.70	0.44
Mapping match, M	–	0.23	0.23	0.24	0.25	0.27	0.30	0.56
Landslide area in Map B	%	10.14	10.47	11.14	11.84	13.63	17.35	48.38
Landslide area in Map C	%	20.87	21.41	22.47	23.54	26.20	31.41	65.81
Map B ∪ Map C	%	23.15	23.72	24.86	25.98	28.82	34.41	69.03
Map B ∩ Map C	%	7.88	8.17	8.77	9.38	10.99	14.44	45.14
Mapping error, E	–	0.66	0.65	0.65	0.64	0.62	0.58	0.35
Mapping match, M	–	0.34	0.35	0.35	0.36	0.38	0.42	0.65

Mapping error, *E*, and mapping match, *M*, computed from Eqs. (1) and (2), respectively.
Map A, reconnaissance landslide inventory prepared by Guzzetti and Cardinali (1989, 1990) (Fig. 3C). Map B, geomorphological landslide inventory prepared by Antonini et al. (2002a) (Fig. 3D). Map C, multi-temporal inventory map (Fig. 4).

estimated age, activity, depth, and velocity. Landslide type was defined according to Cruden and Varnes (1996). Adopting the same procedure used to prepare the detailed geomorphological inventory (Map B), for deep-seated slope failures the landslide crown was mapped separately from the deposit. The distinction was not made for shallow landslides. Landslide age, activity, depth, and velocity were determined based on the type of movement, the morphological characteristics and appearance of the landslides on the aerial photographs, the local lithological and structural setting, and the date of the aerial photographs. Landslide age was defined as recent, old or very old, despite ambiguity in the definition of the age of a mass movement based on its appearance (McCalpin, 1984; Wieczorek, 1984).

The multi-temporal inventory map for the Collazzone area shows 2564 landslides, for a total mapped landslide area of 22.14 km^2 (Table 2), which corresponds to a landslide density of 32.5 slope failures per square kilometre. Due to geographical overlap of landslides of different periods, the total area affected by landslides is 16.47 km^2, 20.87% of the territory. Mapped landslides extend in size from 78 m^2 to 1.45 km^2, and the most abundant failures shown in the map have an area of about 815 m^2 (Table 3).

We refer to the multi-temporal landslide inventory map for the Collazzone area as "Map C".

4. Comparison of the landslide inventory maps

We now compare the landslide inventory maps in the Collazzone area. We perform four tests. The first test aims at evaluating the degree of cartographic matching between the maps, and consists of making "pair-wise" (in pairs) comparisons of the mapped landslides in a GIS. The second test compares the geographical abundance of landslides in the three inventories. Comparison is accomplished by computing the proportion of landslide area in pre-defined terrain units. The third test compares the frequency-area statistics of landslides obtained from the different inventories. The last test evaluates landslide susceptibility assessments obtained using the three inventory maps.

4.1. Direct map comparison

Table 3 summarizes descriptive statistics for the three inventory maps in the Collazzone area, and reveals an increase in the number of landslides with enhanced accuracy of the mapping. The detailed geomorphological inventory (Map B) shows 44.6% of the total number of landslides shown in the multi-temporal inventory (Map C). The percentage reduces to 5.6% for the reconnaissance inventory (Map A). Results are different if the area of the mapped landslides is considered. The geomorphological inventory (Map B) shows 48.6% (8.00 km^2) and the reconnaissance inventory (Map A) shows 47.1% (7.75 km^2) of the total area covered by landslides (16.47 km^2) in the multi-temporal inventory (Map C). The disparity in the number and in the area of the mapped landslides indicates that differences exist in the average size of the slope failures shown in the three inventories (Table 3). The average landslide area in Map A (78,287 m^2) is approximately 10 times larger that the average landslide area shown in Map B (7526 m^2) and

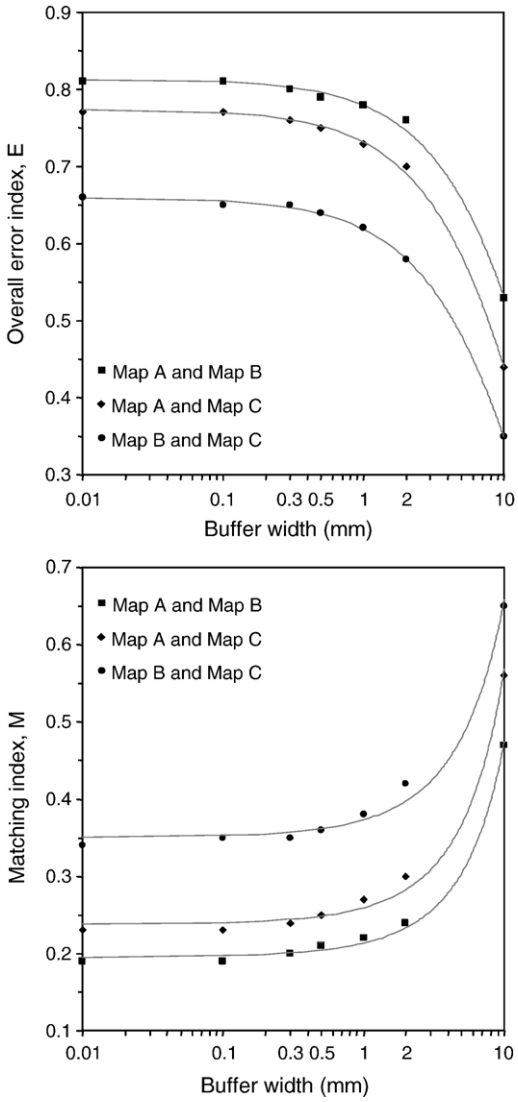

Fig. 5. Estimate of overall mapping error (E) and matching (M) indices for three pair-wise combinations of landslide inventory maps. Lines show exponential fits to the data (least square method).

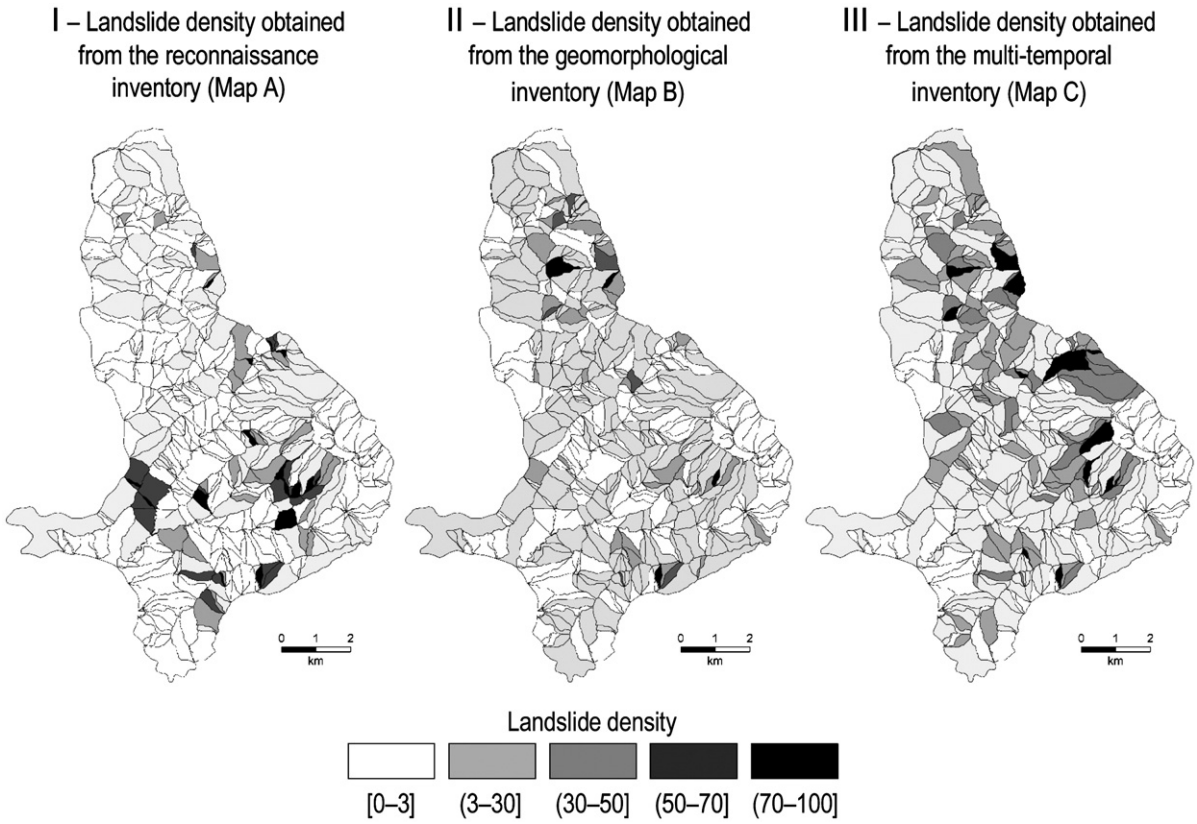

Fig. 6. Landslide density maps for the Collazzone area. Density computed within slope units. Slope units with a percentage of landslide area of less than 3% are considered stable and shown in white. Square bracket indicates class limit is included, round bracket indicates class limit is not included.

in Map C (8634 m^2). When compared to Map B, the slightly larger extent of the average landslide area shown in Map C is due to the presence of a few very large landslides (area >1 km^2), erroneously not shown in the geomorphological inventory (Map B).

The mean area may not be a reliable statistic to compare populations of landslides (Stark and Hovius, 2001; Guzzetti et al., 2002). Table 3 shows that the area of the most abundant (i.e., most frequent) landslides decreases with the increase in the completeness of the inventories. The area of the most abundant landslide is ~32,000 m^2 for the reconnaissance inventory (Map A), ~1170 m^2 for the geomorphological inventory (Map B), and ~815 m^2 for the more accurate multi-temporal inventory (Map C).

To quantify the geographical discrepancy between the three inventories, we adopt the method proposed by Carrara et al. (1992), and we compute the overall error index

$$E = \frac{(A_1 \cup A_2) - (A_1 \cap A_2)}{(A_1 \cup A_2)}, 0 \le E \le 1 \quad (1)$$

where A_1 and A_2 are the total landslide area in the first and in the second inventory, respectively, and $\cup$ and $\cap$ are the geographical union and intersection of the two inventories, easily obtained in a GIS. From Eq. (1), the degree of matching, M, between two inventory maps is

$$M = 1 - E, 0 \le M \le 1. \quad (2)$$

If two inventory maps show exactly the same landslides in the same positions (a rather improbable situation) matching is perfect ($M=1$) and error is nil ($E=0$). If two landslide maps disagree completely, cartographic matching is nil ($M=0$) and error is maximum ($E=1$).

In the GIS, we performed pair-wise geographical union and intersection of the three inventory maps. The obtained figures were used to compute the error (E) and matching (M) indexes. Results are summarized in Table 4. Mapping error ranges from 0.66 to 0.81, which corresponds to a degree of matching in the range between 0.34 and 0.19, respectively. Overall mapping error is smallest (0.66) when the most accurate (Map C)

Table 5
Comparison of stable and unstable slope units based on landslide density computed for the three landslide inventory maps available for the Collazzone area

		Density Map I (obtained from Map A)	
		Stable (358)	Unstable (156)
Density Map II (obtained from Map B)	Stable (255)	213	42
	Unstable (259)	145	114
Disagreement between density maps I and II = 62.12%			

		Density Map I (obtained from Map A)	
		Stable (358)	Unstable (156)
Density Map III (obtained from Map C)	Stable (153)	139	14
	Unstable (361)	219	142
Disagreement between density maps I and III = 62.13%			

		Density Map II (obtained from Map B)	
		Stable (255)	Unstable (259)
Density Map III (obtained from Map C)	Stable (153)	142	11
	Unstable (361)	113	248
Disagreement between density maps II and III = 33.33%			

Stable slope units have a percentage of landslide area of less than 3 percent. Figures in the tables indicate number of terrain units.

and the second most accurate (Map B) inventories are compared.

Eqs. (1) and (2) provide estimates of the mismatch between two landslide maps that encompass all errors associated with the production of the inventories. These errors include: (i) uncertainties associated with the identification of the landslides, (ii) drafting and positional errors introduced when transferring the landslide information from the aerial photographs to the base map, (iii) digitization errors and other mistakes introduced in the construction of the digital cartographic database (Carrara et al., 1992).

We attempt to separate the drafting and digitization errors from the mismatch due to different geomorphological interpretations by drawing buffers of increasing sizes around the mapped landslides. In the GIS, we draw buffers of 1 m, 3 m, 5 m, 10 m, 20 m and 100 m around the landslides shown in Map B and Map C, which were prepared at 1:10,000 scale, and buffers of 2.5 m, 7.5 m, 12.5 m, 25 m, 50 m and 250 m around the landslides shown in Map A, which was prepared at 1:25,000 scale. The selected buffers correspond to 0.1 mm, 0.3 mm, 0.5 mm, 1.0 mm, 2.0 mm and 10 mm, respectively, on the base maps used to show the landslide information. Results are shown in Table 4. With increasing buffer size, mapping error first decreases at a slow rate and then, for large buffers, it decreases rapidly (Fig. 5). Conversely, map matching first increases slowly and then rapidly. We consider the geometric error associated with inaccuracy in transferring the landslide information from the aerial photographs to the base maps and to the digitization errors accounted for by a buffer of about 10 m for the 10,000 scale maps (1 mm for Maps B and C), and by a buffer of about 50 m for the 25,000 scale map (2 mm for Map A). These figures correspond to a cartographic error of approximately 2.5–5%. We attribute the remaining mismatch (~62–75%) to different geomorphological interpretations (Carrara et al., 1992).

4.2. Comparing landslide abundance

A different way of comparing landslide maps consists in comparing the abundance of slope failures in the inventories. To obtain this for the three inventories, we first subdivide the Collazzone study area into terrain units, i.e. distinctly delimited portions of the terrain that contain a set of conditions that differ from the adjacent units across definable boundaries (Guzzetti et al., 1999). We establish the terrain subdivisions using specialised

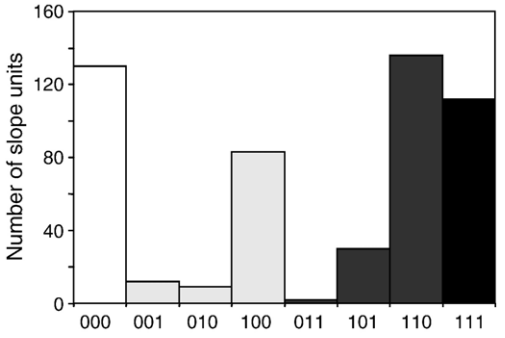

Fig. 7. Comparison of stable (0) and unstable (1) slope units based on landslide density. Stable terrain units have a percentage of landslide area of less than 3%. In the legend of the vertical bars, the left digit refers to the multi-temporal inventory (Map C), the central digit refers to the geomorphological inventory (Map B), and the right digit refers to the reconnaissance inventory (Map A).

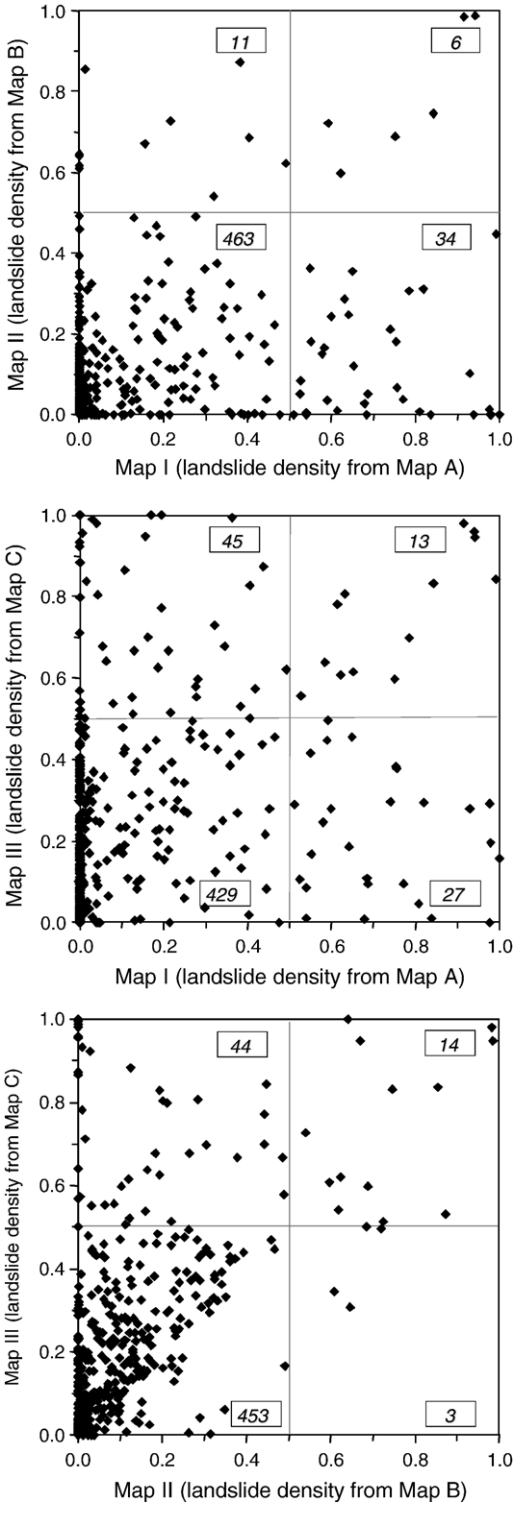

Fig. 8. Comparison of landslide density in the slope units (see Fig. 6).

software that, starting from a 10 m × 10 m DTM, automatically generated drainage and divide lines. By combining the drainage and divide lines, the software identified 514 elementary slope units (Carrara et al., 1991), which represent the terrain units of reference. For each terrain unit, in the GIS we then computed the percentage of landslide area (i.e., the density) shown in the three inventories. Results are shown in Fig. 6, which reveals that the geographical distribution of landslide density varies considerably for the three inventory maps.

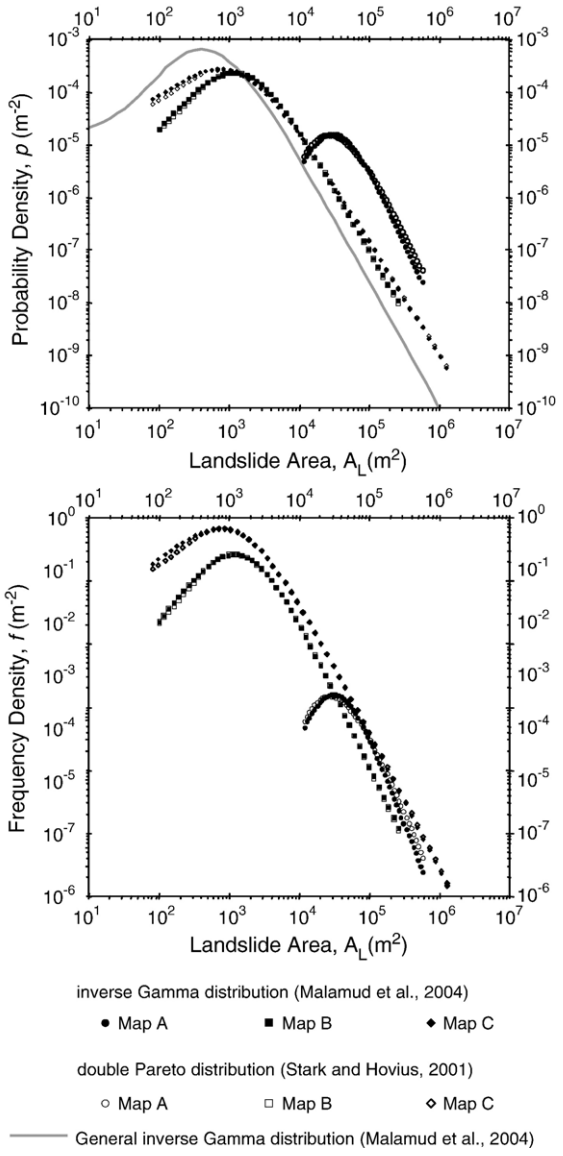

Fig. 9. Statistics of landslide area obtained from the three inventory maps. Upper graph shows dependence of the landslide probability density on landslide area; lower graph shows dependence of the landslide frequency density on landslide area.

Table 6
Comparison of the frequency statistics of landslide area

	Double Pareto Stark and Hovius (2001)	Truncated inverse Gamma Malamud et al. (2004)
$\alpha+1$		
Map A	2.94 (0.218)	2.87 (0.111)
Map B	2.35 (0.055)	2.46 (0.080)
Map C	2.18 (0.034)	2.17 (0.040)
$\bar{A}$ (m^2)		
Map A	32,408	27,664
Map B	1172	1172
Map C	745	908

Values in parenthesis are standard deviation of α. $\bar{A}$ is the size (area) of the most frequent landslide in the estimated distributions.

This is not surprising given the original distribution of the slope failures in the landslide maps (Figs. 3 and 4).

Visual comparison of the density (Fig. 6) and the inventory (Figs. 3C, D and 4) maps, suggests that terrain units having a proportion of landslide area of less than 3% can be considered free of landslides (i.e., stable). This cut-off value was selected to account for drafting and cartographic errors observed by overlaying the individual landslide maps on the slope units map. Typically, the error is represented by a small portion of a landslide deposit crossing a stream line. In Fig. 6, there are 358 stable slope units in the density map obtained from Map A, 255 stable units in the density map obtained from Map B, and 153 stable units in the density map obtained from Map C. We attribute the reduction in the number of stable terrain units to a greater accuracy of the landslide mapping, which resulted in the identification of a larger number of mass movements.

We can compare quantitatively the degree of matching between the three density maps by constructing pair-wise contingency tables (Table 5). The least disagreement (33.3%) is obtained comparing the densities obtained from the "best" (Map C) and the second "best" (Map B) landslide maps, respectively. The comparison outlines a similarity between the two density maps. Mismatch between Map I and Map II, and between Map I and Map III are very similar (~62%), confirming that the density map obtained from the reconnaissance inventory (Map A) is substantially

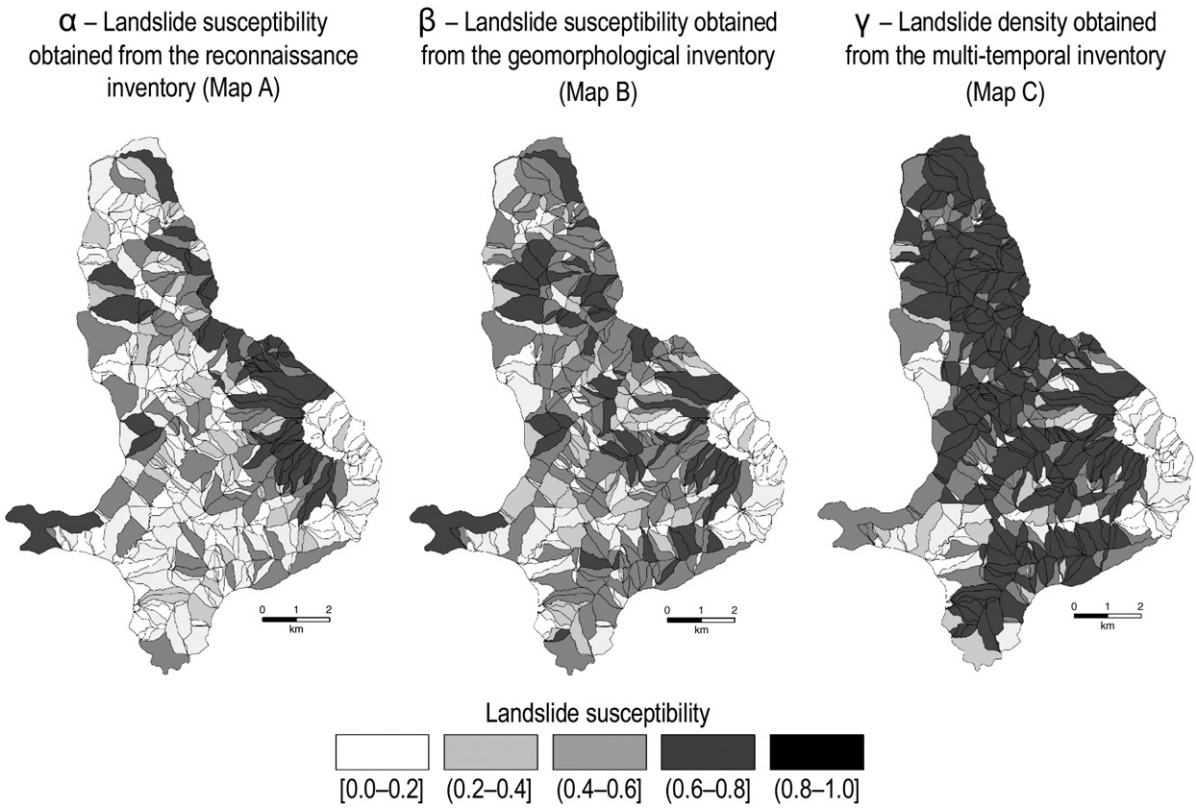

Fig. 10. Landslide susceptibility models for the Collazzone area. Models prepared using the same set of independent thematic variables and three different landslide inventory maps. Square bracket indicates class limit is included, and round bracket indicates class limit is not included.

different from the other two density maps. Fig. 7 summarizes the performed comparisons. There are 242 terrain units (47.1%) classified as stable (130 slope units, 25.3%) or unstable (112 slope units, 21.8%) by all three density maps. These terrain units represent perfect agreement between the different density assessments. There are 429 slope units (83.5%) for which the density obtained from Map A or Map B is in agreement with the density obtained from Map C.

We can further analyse the percentage of landslide area attributed to each slope unit by the individual density maps (Fig. 8). Comparison of the density obtained from the "best" (Map C) and the "poorest" (Map A) landslide maps results in the largest scatter (central graph in Fig. 8). A considerable number of slope units exhibiting a small density of landslides in Map I show a large proportion of landslides in Map III, and *vice versa*. We take this as an indication that the geographical distribution of the landslides shown in the two inventories is considerably different. Comparison of the density Map II (obtained form the geomorphological inventory) with the density Map III (obtained form the multi-temporal inventory) indicates that the differences are largely due to the absence in the geomorphological inventory of a few large and very large landslides (see also Figs. 3D and 4A).

4.3. Comparison of the frequency-area statistics of landslides

Landslide inventory maps can be used to determine the frequency-area statistics of landslides. Several investigators have shown that landslide abundance increases with landslide area up to a maximum value, where landslides are most frequent, and then it decays rapidly (Pelletier et al., 1997; Stark and Hovius, 2001; Guzzetti et al., 2002; Brardinoni et al., 2003; Guthrie and Evans, 2004a, 2004b; Malamud et al., 2004). Two distributions have been proposed to model the empirical distributions of the mapped landslides. Stark and Hovius (2001) proposed a "double Pareto" distribution, and Malamud et al. (2004) proposed a "truncated inverse Gamma" distribution.

We use the double Pareto and the truncated inverse Gamma distributions to compare the frequency-area statistics obtained from the three landslide inventories. To accomplish this, we first obtained the area of the individual landslides in the three inventories from the GIS database. Care was taken to calculate the size of each landslide, avoiding topological and graphical problems related to the presence of smaller landslides inside larger mass movements. For Map B and Map C, we merged the crown area and the deposit, and we

Table 7
Comparison of landslide susceptibility models prepared for the Collazzone area using the same set of 46 independent thematic variables and the three different landslide inventory maps

Susceptibility model α, prepared using the reconnaissance inventory (Map A, Fig. 3C)

			Predicted groups (model)	
			Group 0 stable terrain units	Group 1 unstable terrain units
Actual groups (inventory)	Group 0	Terrain units free of landslides in Map A	247 (48.2%)	82 (16.0%)
	Group 1	Terrain units containing landslides in Map A	57 (11.1%)	126 (24.6%)

Overall percentage of terrain units correctly classified = 72.8%

Susceptibility model β, prepared using the geomorphological inventory (Map B, Fig. 3D)

			Predicted groups (model)	
			Group 0 stable terrain units	Group 1 unstable terrain units
Actual groups (inventory)	Group 0	Terrain units free of landslides in Map B	141 (27.5%)	78 (15.2%)
	Group 1	Terrain units containing landslides in Map B	60 (11.7%)	233 (45.5%)

Overall percentage of terrain units correctly classified = 73.1%

Susceptibility model γ, prepared using the multi-temporal inventory (Map C, Fig. 4)

			Predicted groups (model)	
			Group 0 stable terrain units	Group 1 unstable terrain units
Actual groups (inventory)	Group 0	Terrain units free of landslides in Map C	91 (17.8%)	42 (8.2%)
	Group 1	Terrain units containing landslides in Map C	30 (5.9%)	349 (68.2%)

Overall percentage of terrain units correctly classified = 85.9%.

considered the total area of each mapped landslide. We used the obtained list of landslide areas to estimate an empirical distribution of the landslide areas. Results are shown in Fig. 9 and summarized in Table 6, which shows that the "double Pareto" distribution of Stark and Hovius (2001) and the "truncated inverse Gamma" distribution of Malamud et al. (2004) provide similar results for the three datasets.

The probability density function (*pdf*) obtained from the reconnaissance inventory (Map A) differs significantly from the *pdf* obtained from the other landslide maps. The reconnaissance mapping severely underestimates the number of small and medium sized landslides. This is confirmed by the area of the most abundant landslide shown in Map A, which is ~32,000 m^2. The figure compares with 815 m^2 (Map C) and 1170 m^2 (Map B) obtained for the more accurate maps (Table 3). The power-law tails of the three distributions, which control the frequency (abundance) of the largest landslides, are also different. The scaling exponent ($\alpha+1$) for Map A is steeper (in the range from 2.87 to 2.94) than the scaling obtained for Map B (2.35 to 2.46) and for Map C (2.17 to 2.18). We attribute the differences to the lack of small and medium size landslides in Map A, and to a very large number of small landslides in Map C.

4.4. Comparison of landslide susceptibility assessments

One of the reasons for preparing a landslide inventory map is to determine landslide susceptibility (Brabb, 1984), so that the relative hazard around the landslides becomes apparent. Many methods have been proposed to ascertain landslide susceptibility (Carrara et al., 1995; Soeters and van Westen, 1996; Chung and Fabbri, 1999; Guzzetti et al., 1999) and most of the proposed methods require a landslide inventory. The quality, reliability and completeness of the landslide inventory affect (i.e., control) the quality of the resulting susceptibility assessment (Carrara et al., 1992; Ardizzone et al., 2002).

Table 8
Variables entered into the discriminant models prepared using the same set of 46 independent thematic variables and the three different landslide inventory maps

	Variable description	SDFC		
		Model α	Model β	Model γ
SLO_ARE	Slope-unit area	0.681		
ELV_STD	Standard deviation of slope-unit elevation	0.471	0.419	−0.665
LNK_ANG	Drainage channel mean slope	0.312		
LINK_LEN	Drainage channel length		0.191	
SLO_LEN	Slope-unit mean length	0.226		
LEN_STD	Standard deviation of slope-unit length	−0.414	0.348	
RET	Slope-unit rectilinear profile	0.184		
SLO_ANG	Slope-unit mean slope angle		0.665	
ANG_STD	Standard deviation of slope-unit slope angle		−0.283	
COC_COV	Concave-convex profile down slope			0.130
CONC	Concave profile down slope			0.234
CONV	Convex profile down slope		0.235	
ALLUVIO	Alluvial deposit		−0.202	0.479
ARGILLA	Clay			−0.160
TRAVERTI	Travertine		−0.161	0.388
AREN	Sandstone	−0.193		
CARBO	Limestone	−0.292	−0.703	0.906
MARNE	Marl	0.369		
FRA_OLD	Very old landslides	0.315		
BOSCO	Forested area	−0.325		
URB	Urban area	−0.202		
PASCOLO	Pasture		0.172	
SS	Cultivated area		0.399	
FRA	Bedding dipping away from the slope free face	0.211	0.148	
TRA	Bedding dipping across the slope free face	0.275		
TR2	Slope-unit aspect facing S-SE	0.178		0.256

The table lists variables selected by three discriminant functions as the best predictors of slope instability. The standardized discriminant function coefficients (SDFC) show the relative importance of each variable as a predictor of slope instability. The sign of the coefficient tells if the variable is positively or negatively correlated to instability.

To establish the capability of the available inventory maps to provide landslide susceptibility, we prepare three statistically-based susceptibility models using the three landslide maps. We use the same terrain subdivisions used to determine landslide density (i.e., 514 slope units), and a common set of 46 thematic independent variables, including morphology and hydrology (26 variables), lithology (9 variables), structure and bedding attitude (3 variables), land use (7 variables), and the presence of very old landslide deposits (1 variable) (Guzzetti et al., 2006a). To determine landslide susceptibility we adopt discriminant analysis, a multivariate technique used for classifying samples into alternative groups based on a set of measurements (Michie et al., 1994; Brown, 1998). Results are shown in Fig. 10 and summarized in Table 7. The overall percentage of slope units correctly classified is 72.8% for the reconnaissance inventory (model α), 73.1% for the geomorphological inventory (model β), and 85.9% for the multi-temporal inventory (model γ). These figures were obtained comparing the number of slope units classified as stable or unstable by the three susceptibility models with the presence or absence of the same landslides used to construct the models (test of model fit, Guzzetti et al., (2006b)). The figures confirm that the use of more accurate landslide information leads to more efficient (better fitting) susceptibility models (Carrara et al., 1992).

Table 8 lists the 26 independent thematic variables selected by the step-wise discriminant functions used to construct the three landslide susceptibility models. The number of variables selected by the step-wise discriminant functions varies. It is largest (15 variables) to predict the distribution of landslides shown in Map A, intermediate (12 variables) to predict the distribution of landslides shown in Map B, and least (only 8 variables) to predict the distribution of landslides shown in Map C. We conclude that the use of accurate landslide information reduces the need for thematic data to efficiently predict landslide susceptibility.

We can perform pair-wise comparisons of the landslide susceptibility levels attributed to each slope unit by the individual susceptibility maps (Fig. 11). The best agreement is achieved when model β and model γ are compared, i.e., the susceptibility assessment obtained for the "best" (Map C) and the second "best" (Map B) inventories (lower graph in Fig. 11). In this comparison, 402 slope units (78.2%) are considered similarly (i.e., susceptible (266 units, 51.8%) or not susceptible (136 units, 26.5%)), and 112 slope units (21.8%) are classified differently by the two models. In general, model γ provides larger estimates of landslide susceptibility, a result of the larger number of landslides shown in Map C. Comparison of the susceptibility models obtained from the "poorest" (Map A) and the

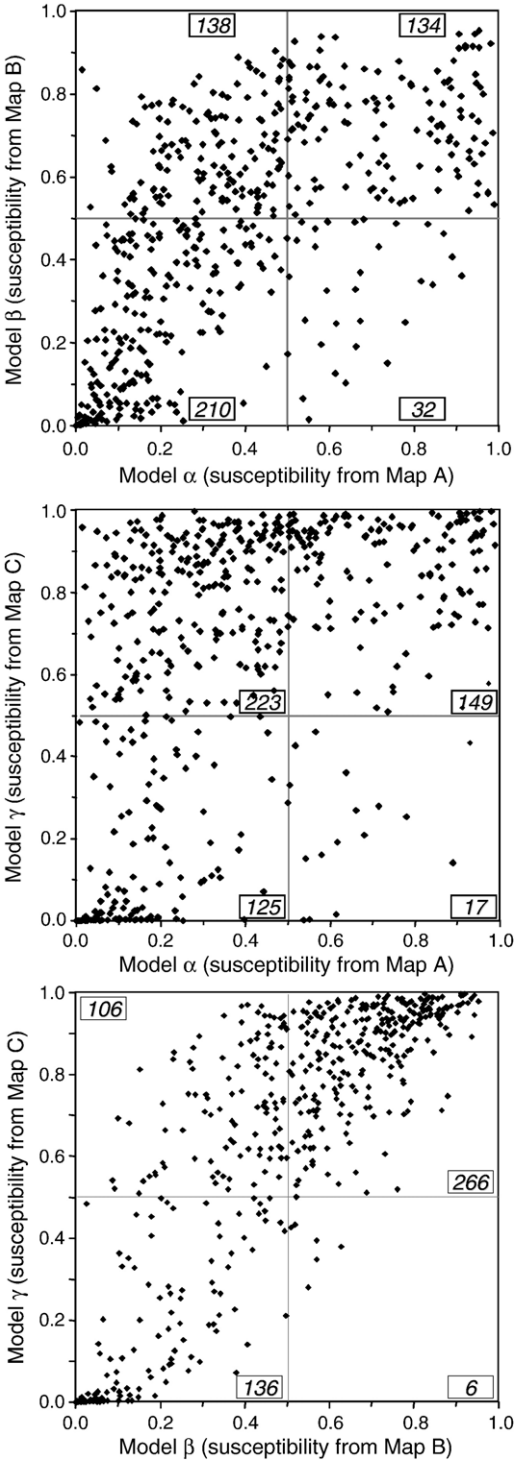

Fig. 11. Comparison of landslide susceptibility estimates for the slope units (see Fig. 10).

"best" (Map C) landslide maps (i.e., model α and model γ, respectively) exhibits the least agreement (second graph in Fig. 11). In this case, the number of slope units for which disagreement exists between the susceptibility assessments is larger (274 units, 53.3%) than the number of slope units for which the susceptibility assessments concur (240 units, 46.7%).

To compare the three susceptibility maps we perform a last test, which consists in determining the fitting performance and the prediction skills of the different susceptibility models (Guzzetti et al., 2006b). For the test we assume that the multi-temporal inventory map (Map C) is accurate, and provides a good representation of the distribution and abundance of slope failures in the Collazzone area. To perform the test, in the GIS we calculate the percentage of landslide area shown in Map C which falls in each probability class, as determined by the three different susceptibility models (Fig. 12). In Fig. 12, the upper plot shows the fitting performance for model γ, i.e., the percentage (vertical bars, left *y*-axis) and the cumulative percentage (line, right *y*-axis) of landslide area in Map C in the susceptibility classes obtained from model γ. The large majority of the landslides are found in areas predicted as susceptible or highly susceptible by the model (dark grey bars). This was expected, as we consider model γ efficient. Conversely, only a fraction of the landslides shown in Map C is found in areas predicted as stable by model γ (light grey bars). The other two plots in Fig. 12 measure the prediction skills of the two susceptibility models, i.e., the ability of model α and of model β to predict the landslides shown in the multi-temporal inventory. Inspection of the third plot indicates that model β is capable of predicting a considerable proportion of the landslides shown in the multi-temporal landslide map, albeit the performance is less satisfactory than that for model γ. The second plot shows that a large proportion of landslides portrayed in Map C are found in areas classified as not susceptible or as poorly susceptible by model α, revealing the inefficiency of this model prepared using a reconnaissance inventory to predict the location of landslides shown in the accurate multi-temporal inventory.

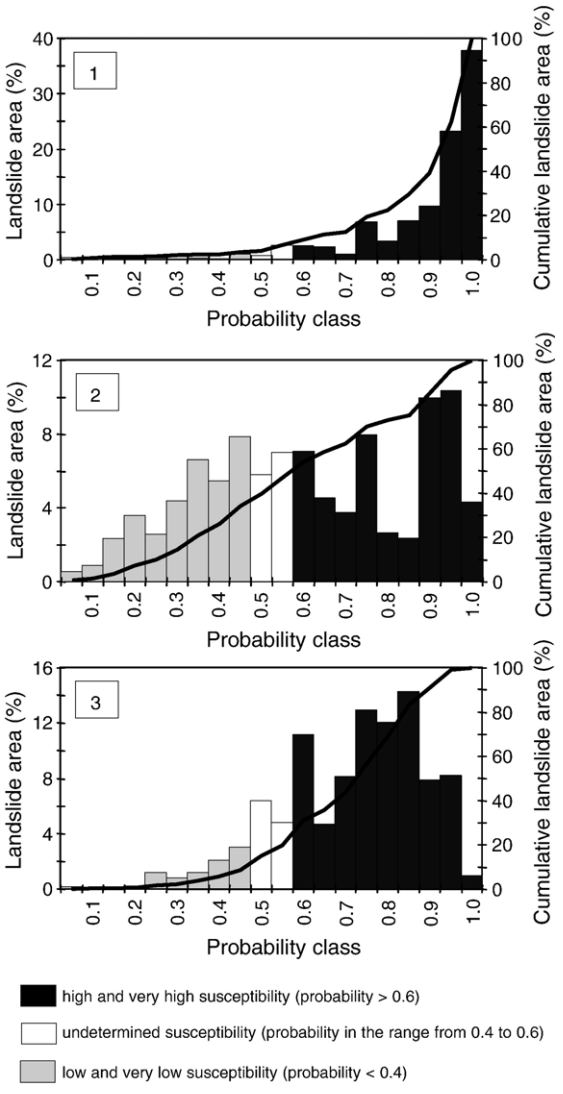

Fig. 12. Model fitting performance (1) and models prediction skill (2 and 3). Graphs show the percentage of landslide area shown in Map C in the susceptibility classes obtained from model γ (1), from model α (2), and from model β (3).

5. Discussion

The availability of three landslide maps for the same area provides the opportunity to compare the inventories and their information content. Results of the comparisons conducted in the Collazzone area allows for: (i) establishing the causes for the mismatch between the three landslide maps, (ii) outlining advantages and limitations of the different techniques used to compile the inventory maps, (iii) estimating the level of completeness of the regional inventories, and (iv) testing the ability of the regional inventories to describe the distribution of slope failures in Umbria, and to assess the landslide susceptibility.

Mismatch between the three landslide maps occurs for many reasons. The different scales of the base maps used to draw the landslides (1:25,000 for Map A, 1:10,000 for Map B and Map C) and of the maps used to construct the GIS database (1:100,000 for Map A,

1:10,000 for Map B and Map C) contributed to the cartographic error, which was largest for the small-scale map (Map A). The type of study (i.e., reconnaissance, geomorphological, multi-temporal), which was a function of the time available for the investigation, were likely to affected the accuracy of the mapping. The experiment suggests that the longer the time available for the investigation, the better the resulting map. The scale, type, date and number of the aerial photographs used to complete the investigations (see Table 1), and the amount of field work associated with the mapping were likely to influence the quality of the inventory maps. Only one set of medium scale aerial photographs was used to compile Map A, two sets of photographs were used to recognize the landslides shown in Map B, and 5 sets of photographs of different dates were used to obtain Map C. The amount of field work was very limited for Map A, limited for Map B, and extensive for Map C. Where field work was performed errors and imprecision were corrected, and the geomorphologists were able to test and refine the photo-interpretation criteria used to recognize and map the landslides from the aerial photographs. The availability of additional geological, morphological and landslide information contributed to the quality of the inventory maps. The information was extremely limited for Map A, abundant for Map B, and very abundant for Map C. The photo-interpretation technique and the experience of the geomorphologists who completed the three inventories improved with time, resulting in more accurate mapping. For the production of the reconnaissance inventory the interpreters based landslide identification solely on the morphological appearance of the landslides. When preparing the geomorphological map, in addition to the morphological appearance of the landslides, the interpreters considered the lithological and structural settings, including the local bedding attitude. For the compilation of the multi-temporal inventory, in addition to the morphological appearance and the local lithological and structural setting, the investigators considered the evolution of the individual landslides. The improved interpretation technique resulted in less interpretation errors and in greater accuracy and completeness of the resulting landslide map. Based on these considerations, we rank the multi-temporal inventory (Map C) the "best" (i.e., the most accurate, complete and reliable) of the three examined landslide maps in the Collazzone area.

The rate of photo-interpretation, which is the average number of square kilometres of an inventory that a single investigator can complete in a unit of time (e.g., a month, Table 2), provides a measure of the resources needed to prepare an inventory. The rate for the multi-temporal mapping (Map C) was 13-time higher than the rate for the geomorphological mapping (Map B), and 60-time higher than the rate for the reconnaissance mapping (Map A). This implies that the team of two geomorphologists that completed the multi-temporal inventory map for the Collazzone area (78.89 km^2) in 5 months, would need 45 years to cover the Umbria region (8456 km^2), assuming the team uses the same technique and the same sets of aerial photographs. The figure compares with the 28 months needed by a team of 3 geomorphologists to complete the geomorphological map, and with the 9 months required by a team of 2 interpreters to compile the reconnaissance inventory (Table 2). We conclude that it is not currently feasible to prepare an accurate multi-temporal inventory map for the entire Umbria region. At the regional scale only regional inventories can be obtained. However, detailed geomorphological landslide maps (e.g. Map B) can be prepared for areas extending for several thousands of square kilometres by teams of experienced geomorphologists.

It is recognized that landslide inventories are generally incomplete. Reasons for the incompleteness are manifold, and determining the level of completeness of a landslide map is not an easy task (Malamud et al., 2004). Guzzetti and Cardinali (1989, 1990) did not provide an estimate of the level of completeness of their reconnaissance inventory. Guzzetti et al. (2003) estimate that the geomorphological inventory is substantially complete for landslides larger than about 2 ha. The latter estimate is heuristic, and not supported by quantitative evidence. In the Collazzone area, the reconnaissance map predicts an area of the most frequent landslides 39 times larger than the area obtained from the multi-temporal inventory (32,000 m^2 vs. 815 m^2). In Map A, the average landslide area is 9 times larger than the corresponding area in Map C (78,287 m^2 vs. 8634 m^2). Lastly, the reconnaissance map predicts a much smaller number of very large landslides. The latter is a consequence of the slope (i.e., the scaling) of the tail of the probability density functions shown in Fig. 9, which for Map A ($\sim$2.90) is appreciably larger than for Map C ($\sim$2.18). When Map B and Map C are compared, the predicted size of the average landslide is marginally smaller (7526 m^2 vs. 8634 m^2), the size of the most abundant landslide is slightly larger (1170 m^2 vs. 815 m^2), and the abundance of the very large landslides is somewhat smaller (the scaling exponent is $\sim$2.40) in the geomorphological inventory.

These figures demonstrate that the reconnaissance mapping severely underestimates the distribution of landslides of many sizes in the Collazzone area. The

figures further indicate that the geomorphological inventory predicts reasonably well the frequency distribution of landslides, at least in the range from about 5000 m^2 to about 200,000 m^2. Outside this range, Map B underestimates the frequency of landslides. Based on the multi-temporal mapping, in the Collazzone area there are 1731 (68%) landslides with an area smaller than 5000 m^2 and 5 (0.2%) landslides with an area larger than 200,000 m^2.

The density (Fig. 6) and the susceptibility (Fig. 10) maps obtained from the three landslide inventories provide different descriptions of the propensity of the Collazzone area to experience new or reactivated landslides. Assuming that the landslide density obtained from the multi-temporal map is a reliable description of the abundance of slope failures in the study area, comparison with the other density maps reveals that the geomorphological inventory provides a more accurate description of landslide abundance than the reconnaissance mapping (Fig. 8). Evaluation of the susceptibility models gives similar results. The landslide susceptibility estimate obtained using the multi-temporal map (model γ, i.e. the "best estimate") is more similar to the estimate obtained from the geomorphological map (model β) than the estimate obtained from the reconnaissance map (model α). Assuming model γ is a reliable representation of landslide susceptibility in the Collazzone area, we conclude that model β is a reasonable proxy for landslide susceptibility in the study area, even if it underestimates the probability of landslide occurrence in a certain number of slope units. Model α provides a less reliable representation of landslide susceptibility, and should not be considered adequate (Fig. 12).

Comparison of the statistics of landslide size, of the distribution of landslide abundance, and of the estimates of landslide susceptibility in the Collazzone area, provide for evaluating the quality and usefulness of the two regional inventories. The reconnaissance inventory offers an insufficient description of the frequency-area distribution of landslides in the Collazzone area. We conclude that similar statistics obtained from the reconnaissance inventory for the entire Umbria region cannot be considered adequate, as they most probably severely underestimate the frequency of landslides of different sizes. On the other hand, the frequency-area statistics obtained from the geomorphological inventory are reasonably accurate in the Collazzone area. We consider this an indication that the same statistics obtained from the geomorphological inventory for the Umbria are adequate.

Similar considerations can be made for the density calculations and for the susceptibility assessments. Based on the tests performed in the Collazzone area, the geomorphological inventory provides realistically accurate landslide information to evaluate landslide density and to assess landslide susceptibility in Umbria. This is a relevant conclusion that suggests that regional susceptibility assessments – such as the "Landslide hazard map for the Upper Tiber River basin", which was prepared using a geomorphological inventory similar to the geomorphological inventory used in this work (Cardinali et al., 2002a) – are reliable and potentially useful products. On the other hand, regional susceptibility models prepared using the reconnaissance landslide maps (e.g. Guzzetti et al., 1999) may not be adequate, and should be used with care.

Susceptibility, the probability of spatial occurrence of landslides, is one of three components of a landslide hazard assessment. To obtain landslide hazard, the temporal probability of landslides, and the probability of landslide size must also be determined. The latter is a proxy for landslide magnitude. Guzzetti et al. (2005, 2006a) have shown how to obtain the required information from an accurate multi-temporal inventory map. At the regional scale, the spatial probability of landslide occurrence, and the probability of landslide size, can be obtained from detailed geomorphological inventories. However, the temporal probability (the expected recurrence) of landslides cannot be obtained from a geomorphological landslide map. This limits the possibility of preparing fully probabilistic landslide hazard assessments at the regional scale.

The size and abundance of landslides, and the propensity of an area to generate new or reactivated landslides, depend on a number of factors, including morphology and lithology. We emphasize that the estimates of landslide size, of landslide density, and of landslide susceptibility obtained from the geomorphological mapping can be considered reliable proxies of the "true" estimates only where morphology and rock types similar to those present in the Collazzone area are present. Where morphology and lithology are substantially different, the correspondence between local and regional estimates will need to be established.

Based on the results obtained in the Collazzone area, and assisted by the limited literature on the assessment of landslide inventory maps (e.g. Roth, 1983; Carrara et al., 1992; van Westen et al., 1999; Ardizzone et al., 2002), we now propose a general framework for the quantitative comparison of landslide inventory maps. Where two (or more) inventory maps are available for the same area, we recommend that the maps be compared to assess: (i) the extent of the cartographic matching between the maps, (ii) the differences in the

abundance and distribution of the mapped landslides, (iii) the frequency-size (i.e., area, volume) statistics of the mapped landslides, and (iv) the performance of the inventory maps as predictors of landslide susceptibility.

Pair-wise analysis of the mapped landslides in a GIS allows for testing the degree of cartographic agreement (or disagreement) between two maps. To quantify the geographical correspondence, the error and the matching indices can be used. Drawing confidence areas of different sizes around the mapped landslides helps determining the proportion of the mismatch due to drafting and other cartographic errors and the errors associated with the construction of the GIS database, from map differences due to diverse geomorphological interpretations. Simple geographical operations in a GIS allow for quantifying the differences in the abundance of the mapped landslides. For the purpose, a geomorphologically meaningful subdivision of the terrain is required. Slope units demonstrated to be particularly suited for the scope, but other terrain subdivisions can be adopted (Guzzetti et al., 1999). To summarize the differences, contingency tables and specific plots can be prepared. The frequency-area statistics of landslides can be obtained from digital catalogues of landslide areas. In preparing the catalogues, care must be taken in defining the area of the individual landslides. Estimating the probability density or the frequency density of landslide area from an empirical distribution is not a trivial exercise. Care must be taken in the application of the obtained statistics, considering the errors (i.e. the levels of uncertainty) associated with the statistics. Lastly, the significance of a landslide map as a source of information to assess landslide susceptibility can be established by comparing the susceptibility model prepared using the map to be tested against a second susceptibility model prepared using the same set of thematic data and more reliable landslide information. Again, to summarize the differences between susceptibility models, contingency tables and plots can be prepared. To facilitate the comparisons, susceptibility models should be prepared – and compared – using the same terrain subdivisions used to compare landslide density maps.

6. Concluding remarks

Landslide maps contain important information to investigate the evolution of landforms, and to ascertain landslide susceptibility and hazards. Landslide inventory maps are effective and intelligible products for experts and non experts, including decision-makers, planners, civil defense managers, and concerned citizens. Due to the techniques used to compile the inventory maps, landslide inventories are subjective products, whose quality depends on the skill and the experience of the investigators, the complexity of the study area, and the completeness and reliability of the available information, including the aerial photographs used to identify the landslides (Guzzetti et al., 2000; Malamud et al., 2004).

Despite their relevance, comparatively little effort is made to assess the quality of landslide maps. To address this problem, we have proposed a general framework for the quantitative and objective comparison of landslide inventory maps. The framework consists of a set of tests, and is based on the experience gained in 20 years of landslide mapping in central Italy (Guzzetti and Cardinali, 1989, 1990; Antonini et al., 1993; Cardinali et al., 2000, 2001, 2002a,b; Antonini et al., 2002a,b; Guzzetti et al., 2005), and on the existing literature on the assessment of the quality of landslide maps (Roth, 1983; Carrara et al., 1992; van Westen et al., 1999; Ardizzone et al., 2002). In the proposed framework, the tests are designed to assess specific aspects of the quality of a landslide map, and to compare the quality of two or more maps.

We have evaluated the proposed framework in the Collazzone area, in central Umbria, an area for which three different inventory maps are available. Results showed that a multi-temporal inventory prepared through the systematic and simultaneous interpretation of several sets of aerial photographs of different vintages, supplemented by extensive geological and geomorphological field surveys, is superior to (i.e., more reliable than) geomorphological or reconnaissance inventories prepared for the same area. However, due to the time and the resources required to complete a multi-temporal inventory, such type of detailed mapping cannot be effectively prepared for a large region, extending for thousands of square kilometres. At the regional scale, detailed geomorphological inventories prepared by teams of experienced geomorphologists provide a reasonable alternative to multi-temporal landslide maps.

Finally, we think that the proposed framework, if broadly adopted, will provide for quantitative comparisons of landslide inventory maps prepared by different investigators working in the same area. Ultimately, this will provide useful information to establish the reliability and cost effectiveness of the different methods used to prepare landslide inventory maps. This will contribute to establish quality criteria and standards for landslide inventory map, and may prove particularly significant in view of the exploitation of new, very high resolution satellite imagery to recognize and monitor the landslides.

Acknowledgments

We are grateful to Earl Brabb and an anonymous referee for the constructive comments. This research is supported by CNR IRPI funds. CNR GNDCI publication number 2895.

References

Antonini, G., Cardinali, M., Guzzetti, F., Reichenbach, P., Sorrentino, A., 1993. Carta Inventario dei Fenomeni Franosi della Regione Marche ed aree limitrofe. CNR Gruppo Nazionale per la Difesa dalle Catastrofi Idrogeologiche Publication n. 580, 2 sheets, scale 1:100,000, (in Italian).

Antonini, G., Ardizzone, F., Cacciano, M., Cardinali, M., Castellani, M., Galli, M., Guzzetti, F., Reichenbach, P., Salvati, P., 2002a. Rapporto Conclusivo Protocollo d'Intesa fra la Regione dell'Umbria, Direzione Politiche Territoriali Ambiente e Infrastrutture, ed il CNR–IRPI di Perugia per l'acquisizione di nuove informazioni sui fenomeni franosi nella regione dell'Umbria, la realizzazione di una nuova carta inventario dei movimenti franosi e dei siti colpiti da dissesto, l'individuazione e la perimetrazione delle aree a rischio da frana di particolare rilevanza, e l'aggiornamento delle stime sull'incidenza dei fenomeni di dissesto sul tessuto insediativo, infrastrutturale e produttivo regionale. Unpublished report, May 2002, 140 pp., (in Italian).

Antonini, G., Ardizzone, F., Cardinali, M., Galli, M., Guzzetti, F., Reichenbach, P., 2002b. Surface deposits and landslide inventory map of the area affected by the 1997 Umbria–Marche earthquakes. Bollettino Società Geologica Italiana 121 (2), 843–853.

Ardizzone, F., Cardinali, M., Carrara, A., Guzzetti, F., Reichenbach, P., 2002. Uncertainty and errors in landslide mapping and landslide hazard assessment. Natural Hazards and Earth System Sciences 2 (1–2), 3–14.

Barchi, M., Brozzetti, F., Lavecchia, G., 1991. Analisi strutturale e geometrica dei bacini della media valle del Tevere e della valle umbra. Bollettino Società Geologica Italiana 110, 65–76 (in Italian).

Barchi, M., Cardinali, M., Guzzetti, F., Lemmi, M., 1993. Relazioni fra movimenti di versante e fenomeni tettonici nell'area del M. Coscerno – M. di Civitella, Val Nerina (Umbria). Bollettino Società Geologica Italiana 112, 83–111 (in Italian).

Brabb, E.E., 1984. Innovative approaches to landslide hazard mapping. Proceedings 4th International Symposium on Landslides, Toronto vol. 1, 307–324.

Brabb, E.E., Harrod, B.L. (Eds.), 1989. Landslides: Extent and Economic Significance. Balkema Publisher, Rotterdam. 385 pp.

Brardinoni, F., Slaymaker, O., Hassan, M.A., 2003. Landslide inventory in a rugged forested watershed: a comparison between air-photo and field survey data. Geomorphology 54 (3-4), 179–196.

Brown, C.E., 1998. Applied Multiple Statistics in Geohydrology and Related Sciences. Springer-Verlag. 248 pp.

Bucknam, R.C., Coe, J.A., Chavarria, M.M., Godt, J.W., Tarr, A.C., Bradley, L.-A., Rafferty, S., Hancock, D., Dart, R.L., Johnson, M.L., 2001. Landslides triggered by hurricane mitch in Guatemala — inventory and discussion. U.S. Geological Survey Open File Report 01–443. 38 pp.

Cardinali, M., Galli, M., Guzzetti, F., Reichenbach, P., Borri, G., 1994. Relazioni fra movimenti di versante e fenomeni tettonici nel bacino del Torrente Carpina (Umbria settentrionale). Geografia Fisica e Dinamica Quaternaria 17, 3–17 (in Italian).

Cardinali, M., Ardizzone, F., Galli, M., Guzzetti, F., Reichenbach, P., 2000. Landslides triggered by rapid snow melting: the December 1996–January 1997 event in Central Italy. In: Claps, P., Siccardi, F. (Eds.), Proceedings 1st Plinius Conference, Maratea. Bios Publisher, Cosenza, pp. 439–448.

Cardinali, M., Antonini, G., Reichenbach, P., Guzzetti, F., 2001. Photo–geological and landslide inventory map for the Upper Tiber River basin. CNR Gruppo Nazionale per la Difesa dalle Catastrofi Idrogeologiche Publication n. 2154, scale 1:100,000.

Cardinali, M., Carrara, A., Guzzetti, F., Reichenbach, P., 2002a. Landslide hazard map for the Upper Tiber River basin. CNR Gruppo Nazionale per la Difesa dalle Catastrofi Idrogeologiche Publication n. 2116, scale 1:100,000.

Cardinali, M., Reichenbach, P., Guzzetti, F., Ardizzone, F., Antonini, G., Galli, M., Cacciano, M., Castellani, M., Salvati, P., 2002b. A geomorphological approach to estimate landslide hazard and risk in urban and rural areas in Umbria, central Italy. Natural Hazards and Earth System Sciences 2 (1–2), 57–72.

Carrara, A., Cardinali, M., Detti, R., Guzzetti, F., Pasqui, V., Reichenbach, P., 1991. GIS techniques and statistical models in evaluating landslide hazard. Earth Surface Processes and Landform 16 (5), 427–445.

Carrara, A., Cardinali, M., Guzzetti, F., 1992. Uncertainty in assessing landslide hazard and risk. ITC Journal 2, 172–183.

Carrara, A., Cardinali, M., Guzzetti, F., Reichenbach, P., 1995. GIS technology in mapping landslide hazard. In: Carrara, A., Guzzetti, F. (Eds.), Geographical Information Systems in Assessing Natural Hazards. Kluwer Academic Publisher, Dordrecht, pp. 35–175.

Cencetti, C., 1990. Il Villafranchiano della "riva umbra" del F. Tevere: elementi di geomorfologia e di neotettonica. Bollettino Società Geologica Italiana 109 (2), 337–350 (in Italian).

Conti, M.A., Girotti, O., 1977. Il Villafranchiano nel "Lago Tiberino", ramo sud–occidentale: schema stratigrafico e tettonico. Geologia Romana 16, 67–80 (in Italian).

Chung, C.J., Fabbri, A.G., 1999. Probabilistic prediction models for landslide hazard mapping. Photogrammetric Engineering & Remote Sensing 65 (12), 1389–1399.

Chung, C.J., Fabbri, A.G., 2003. Validation of spatial prediction models for landslide hazard mapping. Natural Hazards 30 (3), 451–472.

Chung, C.J., Fabbri, A.G., 2005. Systematic procedures of landslide hazard mapping for risk assessment using spatial prediction models. In: Glade> (Ed.), Landslide Risk Assessment. John Wiley, pp. 139–174.

Cruden, D.M., Varnes, D.J., 1996. Landslide types and processes. In: Turner, A.K., Schuster, R.L. (Eds.), Landslides, Investigation and Mitigation. Transportation Research Board Special Report, vol. 247. National Academy Press, Washington D.C., pp. 36–75.

DeGraff, J.V., 1985. Using isopleth maps of landslides deposits as a tool in timber sale planning. Bulletin American Association of Engineering Geologists 22, 445–453.

DeGraff, J.V., Canuti, P., 1988. Using isopleth mapping to evaluate landslide activity in relation to agricultural practices. International Association Engineering Geology Bulletin 36, 61–71.

Guthrie, R.H., Evans, S.G., 2004a. Magnitude and frequency of landslides triggered by a storm event, Loughborough Inlet, British Columbia. Natural Hazards and Earth System Sciences 4, 475–483.

Guthrie, R.H., Evans, S.G., 2004b. Analysis of landslide frequencies and characteristics in a natural system, coastal British Columbia. Earth Surface Processes and Landforms 29 (11), 1321–1339.

Guzzetti, F., Cardinali, M., 1989. Carta Inventario dei Fenomeni Franosi della Regione dell'Umbria ed aree limitrofe. CNR Gruppo Nazionale per la Difesa dalle Catastrofi Idrogeologiche Publication n. 204, 2 sheets, scale 1:100,000, (in Italian).

Guzzetti, F., Cardinali, M., 1990. Landslide inventory map of the Umbria region, Central Italy. In: Cancelli, A. (Ed.), Proceedings ALPS 90 6th International Conference and Field Workshop on Landslides, Milan, 12 September 1990, pp. 273–284.

Guzzetti, F., Cardinali, M., Reichenbach, P., 1996. The influence of structural setting and lithology on landslide type and pattern. Environmental and Engineering Geoscience 2 (4), 531–555.

Guzzetti, F., Carrara, A., Cardinali, M., Reichenbach, P., 1999. Landslide hazard evaluation: a review of current techniques and their application in a multi-scale study, Central Italy. Geomorphology 31, 181–216.

Guzzetti, F., Cardinali, M., Reichenbach, P., Carrara, A., 2000. Comparing landslide maps: a case study in the upper Tiber River Basin, Central Italy. Environmental Management 25 (3), 247–363.

Guzzetti, F., Malamud, B.D., Turcotte, D.L., Reichenbach, P., 2002. Power–law correlations of landslide areas in Central Italy. Earth and Planetary Science Letters 195, 169–183.

Guzzetti, F., Galli, M., Reichenbach, P., Ardizzone, F., Cardinali, M., 2006a. Landslide hazard assessment in the Collazzone area, Umbria, central Italy. Natural Hazards and Earth System Sciences 6, 115–131.

Guzzetti, F., Reichenbach, P., Ardizzone, F., Cardinali, M., Galli, M., 2006b. Estimating the quality of landslide susceptibility models. Geomorphology 81, 166–184.

Guzzetti, F., Reichenbach, P., Cardinali, M., Ardizzone, F., Galli, M., 2003. Impact of landslides in the Umbria Region, Central Italy. Natural Hazards and Earth System Sciences 3, 469–486.

Guzzetti, F., Reichenbach, P., Cardinali, M., Galli, M., Ardizzone, F., 2005. Probabilistic landslide hazard assessment at the basin scale. Geomorphology 72, 272–299.

Harmon, R.S., Doe III, W.W., 2001. Landscape Erosion and Evolution Modeling, Spinger-Verlag. 535 pp.

Harp, E.L., Jibson, R.L., 1995. Inventory of Landslides Triggered by the 1994 Northridge, California Earthquake. U.S. Geological Survey Open File Report, pp. 95–213.

Harp, E.L., Jibson, R.L., 1996. Landslides triggered by the 1994 Northridge, California earthquake. Seismological Society of America Bulletin 86, S319–S332.

Hovius, N., Stark, C.P., Allen, P.A., 1997. Sediment flux from a mountain belt derived by landslide mapping. Geology 25, 231–234.

Hovius, N., Stark, C.P., Hao-Tsu, C., Jiun-Chuan, 2000. Supply and removal of sediment in a landslide-dominated mountain belt: Central Rang, Taiwan. The Journal of Geology 108, 73–89.

Lattuada, S., 1996. Relazione tra assetto geologico–morfologico e distribuzione dei movimenti franosi nell'area di Mercatale (AR), caratterizzazione geotecnica delle Argille Varicolori. Unpublished Thesis, Dipartimento di Scienze della Terra, University of Milano, Milano, 152 pp., (in Italian).

Malamud, B.D., Turcotte, D.L., Guzzetti, F., Reichenbach, P., 2004. Landslide inventories and their statistical properties. Earth Surface Processes and Landforms 29 (6), 687–711.

McCalpin, J., 1984. Preliminary age classification of landslides for inventory mapping: 21st Annual Symposium on Engineering Geology and Soils Engineering. Proceedings, University of Idaho, Moscow, ID, pp. 99–111.

Michie, D., Spiegelhalter, D.J., Taylor, C.C. (Eds.), 1994. Machine Learning, Neural and Statistical Classification. Internet version available at http://www.amsta.leeds.ac.uk/~charles/statlog/.

Pelletier, J.D., Malamud, B.D., Blodgett, T., Turcotte, D.L., 1997. Scale-invariance of soil moisture variability and its implications for the frequency-size distribution of landslides. Engineering Geology 48, 255–268.

Reichenbach, P., Galli, M., Cardinali, M., Guzzetti, F., Ardizzone, F., 2005. Geomorphologic mapping to assess landslide risk: concepts, methods and applications in the Umbria Region of central Italy. In: Glade, T., Anderson, M.G., Crozier, M.J. (Eds.), Landslide Risk Assessment. John Wiley, pp. 429–468.

Roth, R.A., 1983. Factors affecting landslide susceptibility in San Mateo County, California. Association Engineering Geologists Bulletin 20 (4), 353–372.

Servizio Geologico Nazionale, 1980. Carta Geologica dell'Umbria. Map at 1:250,000 scale, (legend in Italian).

Soeters, R., van Westen, C.J., 1996. Slope instability recognition, analysis and zonation. In: Turner, A.K., Schuster, R.L. (Eds.), Landslide Investigation and Mitigation, National Research Council. Transportation Research Board Special Report, vol. 247, pp. 129–177.

Stark, C.P., Hovius, N., 2001. The characterization of landslide size distributions. Geophysics Research Letters 28, 1091–1094.

Toppi, A., 1993. Studio geologico–tecnico sullo stato di dissesto del bacino idrografico del F.sso Bianco–T. Caldaro in Provincia di Terni. Unpublished Thesis, Dipartimento di Scienze della Terra, University of Perugia, Perugia, 103 pp., (in Italian).

van Westen, C.J., Seijmonsbergen, A.C., Mantovani, F., 1999. Comparing landslide hazard maps. Natural Hazards 20 (2–3), 137–158.

Varnes, D.J., 1978. Slope movements: types and processes. In: Schuster, R.L., Krizek, R.J. (Eds.), Landslide Analysis and Control, National Academy of Sciences. Transportation Research Board Special Report, vol. 176, pp. 11–33. Washington D.C.

Wieczorek, G.F., 1984. Preparing a detailed landslide-inventory map for hazard evaluation and reduction. Bulletin Association Engineering Geologists 21 (3), 337–342.

WP/WLI – International Geotechnical societies' UNESCO Working Party on World Landslide Inventory, 1990. A suggested method for reporting a landslide. International Association Engineering Geology Bulletin 41, 5–12.